J. Coat. Technol. Res.
https://doi.org/10.1007/s11998-026-01306-9

Acrylated tannic acid as bio-based adhesion promoter for EB-curable coatings

Francesco Bisio, Katia Sparnacci, Gianni Mirone, Stefania Pasquin, Alessandro Nicorelli

Received: 17 November 2025 / Revised: 4 February 2026 / Accepted: 7 February 2026

Abstract Electron beam (EB) curing has emerged as a highly attractive technology for advanced coating systems due to its solvent-free nature, energy efficiency, and ability to initiate polymerization without photoinitiators. This feature minimizes extractable species, a critical advantage for environmental sustainability and food safety. This study investigates partially acrylated tannic acid derivatives (TA–GMx) as bio-based adhesion promoters for EB-curable acrylic coatings in metal packaging applications. Tannic acid was functionalized with glycidyl methacrylate to tailor its polarity and introduce polymerizable groups capable of directly participating in EB-induced crosslinking. The resulting TA–GMx additives, synthesized with varying degrees of acrylation x, were incorporated into an industrial, partially bio-based formulation at different loadings (1.0 and 3.0 wt%). Their influence on network formation and interfacial performance was systematically evaluated. Mechanical and electrochemical tests on various metal substrates demonstrated that the incorporation of TA–GMx additives significantly improved adhesion, flexibility under deformation, and resistance to corrosion-induced delamination. Optimal performance was achieved at 1.0 wt% additive concentrations, where a balance between crosslink density and interfacial interactions was established. These findings highlight the synergy between EB technology and bio-based adhesion promoters as an effective strategy for developing high-performance, sustainable coatings for food metal packaging

Keywords Electron beam (EB) curing, Acrylated tannic acid (TA-GMx), Bio-based adhesion promoters, Metal substrates/packaging, Metal adhesion

Introduction

Polymeric coatings play a pivotal role in protecting and enhancing the functionality of metallic, polymeric and composite substrates. They act as a barrier against corrosion, chemical attack and mechanical damage and also improve surface esthetics and processability. Driven by the need for sustainability, the coating industry has shifted its focus toward high-performance, sustainable systems that minimize volatile organic compounds (VOCs) emissions and energy consumption. Consequently, radiation curing—specifically ultraviolet (UV) and electron beam (EB) technologies—has emerged as a prominent, solvent-free alternative to conventional thermal curing.[1–4] A comparison of these methods highlights the distinct advantages of EB technology. First, by utilizing high-energy electrons to directly initiate polymerization, EB eliminates the need for photoinitiators, avoiding potential migration issues critical in food contact applications.[5] Moreover, EB radiation possesses greater penetrating power than UV photons, ensuring effective curing even in thick or opaque coatings.[6]

This paper was presented at the 20th Coatings Science International Conference held from June 30–July 3, 2025, in Noordwijk, the Netherlands.

F. Bisio (✉), K. Sparnacci (✉)
Dipartimento di Scienze ed Innovazione Tecnologica, Università degli Studi del Piemonte Orientale ''A. Avogadro'' via Michel 11, 15121 Alessandria, Italy
e-mail: francesco.bisio@uniupo.it

K. Sparnacci
e-mail: katia.sparnacci@uniupo.it

F. Bisio, K. Sparnacci
INSTM UdR Alessandria, Alessandria, Italy

G. Mirone, S. Pasquin, A. Nicorelli
METLAC SpA, Strada Provinciale ex strada statale 35 Bis Dei Giovi 53 , 15062 Bosco Marengo, AL, Italy

Published online: 05 June 2026

In the food packaging sector, metallic containers—typically tinplate, tin-free steel, or aluminum—rely on internal and external organic coatings to prevent corrosion and product contamination. Conventional coatings, predominantly based on epoxy–phenolic or polyester resins, are applied via roller (sheet-fed application) or spray coating and require thermal curing to induce crosslinking.[7] While thermally cured systems offer excellent performance, they necessitate high temperatures and prolonged processing times, resulting in substantial energy consumption and the potential degradation of heat-sensitive substrates. Consequently, UV- and EB-curable coatings have emerged as superior alternatives characterized by low energy requirements, minimal VOC emissions, and the capability for fast, in-line processing.[8,9]

Robust adhesion to the metallic substrate is a prerequisite for coatings in metal packaging. Poor interfacial bonding in aggressive environments can result in severe defects, including coating delamination, underfilm corrosion and premature coating failure.[10] Adhesion performance is governed by a complex interplay of factors, including substrate surface chemistry, coating polarity and specific interfacial mechanisms. Therefore, the incorporation of adhesion promoters has become a standard strategy to strengthen polymer–metal interfaces.[11] These agents act as molecular bridges: They possess dual functionalities capable of participating in the coating's crosslinking network while simultaneously forming stable bonds with the metal surface. While traditional promoters such as organosilanes, zirconates, and phosphate esters remain common, research has recently shifted toward bio-inspired strategies.[12–14] In particular, catechol-functionalized compounds, inspired by mussel adhesive proteins, have emerged as promising eco-friendly candidates capable of significantly enhancing metal–polymer interactions through hydrogen bonding and metal chelation.[15–17]

Among naturally derived materials, tannic acid (TA) has garnered significant attention due to its polyphenolic structure. Rich in galloyl and catechol-like moieties, TA can coordinate with metal ions to form robust interfacial interactions.[18–20] Consequently, it has been investigated as a corrosion inhibitor, surface primer, and crosslinking agent in various coating systems. Several studies have highlighted the potential of TA and its derivatives as bio-based adhesion promoters in radiation-curable coatings. For instance, unmodified tannic acid has been employed as an adhesion promoter in cationically polymerized, epoxidized soybean oil-based coatings cured under UV irradiation. In this context, the phenolic groups of TA served dual functions: acting as catalytic centers to enhance epoxy conversion and promoting adhesion to steel through coordination bonding with surface iron ions.[21]

Conversely, the incorporation of tannic acid into an acrylic coating necessitates a chemical modification of the molecule to introduce functional groups capable of participating in the crosslinking reaction of the coating.

The synthesis of multifunctional (meth)acrylated tannic acid derivatives has been extensively investigated to enable the incorporation of tannic acid into radiation-curable coating systems. The most common synthetic approach involves the ring opening reaction between tannic acid and glycidyl (meth)acrylate, yielding derivatives bearing polymerizable double bonds.[22–24] Using this strategy, Liu at al.[22,23] incorporated methacrylated tannic acid into UV-curable formulations based on acrylated epoxidized soybean oil, reporting significant improvements in hardness, adhesion, and tensile strength. Similarly, Wang et al.[24] reported enhanced adhesion of UV-cured coatings on metal substrates through the use of acrylated tannic acid as a bio-based adhesion promoter.

More recently, research has shifted toward sustainable synthesis routes. Notably, microwave-assisted methacrylation has emerged as a rapid, solvent-free method to functionalize tannic acid with a high degree of substitution. This approach has yielded UV-curable coatings characterized by high photo-reactivity, thermal stability, and effective corrosion protection.[25]

While the potential of acrylated tannic acid in UV systems is well documented, its application in electron beam (EB) curing remains less explored. Consequently, this work investigated the efficacy of partially acrylated tannic acid derivatives as a bio-based adhesion promoter in EB-curable coatings.

The acrylation of tannic acid through reaction with glycidyl methacrylate (GMA) was designed to tailor the molecule's polarity, thereby ensuring compatibility with the acrylate matrix while introducing reactive functionalities capable of covalent integration into the network during EB curing.

To this end, three partially acrylated tannic acid derivatives with varying degrees of functionalization, denoted as TA–GMx (where x denotes the degree of functionalization) were prepared. These additives were incorporated into an industrial, partially bio-based EB-curable acrylic system at various loadings. The work systematically assesses the influence of these additives on the overall coating performance, with a particular emphasis on adhesion, mechanical flexibility, and corrosion resistance. The results offer valuable insights into developing sustainable adhesion promoters for the metal packaging industry.

Experimental

Materials

Tannic acid (TA), glycidyl methacrylate (GMA), isobornyl acrylate (IBOA, technical grade), tetrahydrofurfuryl acrylate (THFA), cyclic trimethylolpropane formal acrylate (CTFA), triethylamine (TEA), 2,6-di*tert*butyl-4-methylphenol (BHT), and

acetonitrile (MeCN) were purchased from Sigma-Aldrich and employed without any further purification.

The formulation components were supplied by METLAC SpA: difunctional polyester urethane acrylate (R02), difunctional aliphatic urethane acrylate (G69), tetrafunctional polyester acrylate (R32), along with a silicone-based wetting agent (A84). The metal substrates selected for this study, also supplied by Metlac SpA, were: electrolytic tinplate (ETP), passivated tinplate (ETP ox), Cr-free tinplate (CFPA), low tin steel (LTS) and electrolytic chromium-coated steel (ECCS).

Synthesis of acrylated tannic acid (TA-GMx)

The TA-GMx derivatives were synthesized using a three-necked, round-bottom flask equipped with an addition funnel, a condenser, and a nitrogen inlet. The synthesis procedure was adapted from a previously reported method.[24,25] Three derivatives TA-GM5, TA-GM15 and TA-GM20 were obtained by using different molar ratios between TA and GMA, equal to 5, 15 and 20. Synthetic details are reported in Table 1.

The synthesis of TA-GM15 was described as a typical example: TA (10.2 g, 6.00 mmol), BHT (23 mg, 0.104 mmol), TEA (0.345 g, 3.40 mmol) and a mixture of MeCN and H_2O (15 v/v%) (20 mL) were placed in a 250-mL round-bottom flask and stirred at 80°C until complete dissolution was achieved. GMA (12.79 g, 90.0 mmol) was then added dropwise to the mixture, which was stirred continuously at 80°C for 24 hours. At the end of the reaction, the mixture was concentrated under reduced pressure, yielding a dark brown viscous liquid that was identified as glycidyl methacrylate-modified tannic acid.

Preparation of EB-curable coatings

The modified EB-curable formulations were prepared by incorporating TA–GMx additives into the base acrylic system at loadings of 1 and 3 wt%. The reference formulation has an average acrylate functionality of 2.0 mol per 100 g of the final blend. The addition of TA–GMx additives slightly increases the overall functionality to a value of 2.1–2.4, as calculated for TA-GM15 additive. The detailed composition of each sample is summarized in Table 2.

The liquid formulations were applied onto the selected metallic substrates (ETP, ETP ox, CFPA and LTS) using a wire-wound bar coater (RDS-4 ½''coater, nominal wet film thickness: 9.14 μm). Curing was performed using an EBLab-200 electron beam unit operating at an acceleration voltage of 80 kV, a dose of 40 kGy and a dose rate of 150 kGy•s^{-1}. The metal substrates were employed as received, without prior cleaning or degreasing.

Free-standing films for DMTA analysis were prepared following the same procedure but applied onto electrolytic chromium-coated steel (ECCS). Due to the poor adhesion of the coating to this specific substrate, the cured films could be easily peeled off, allowing for the isolation of free-standing specimens.

Characterization of EB-cured films

The degree of acrylate conversion was analyzed using attenuated total reflectance Fourier-transform infrared spectroscopy (ATR-FTIR) on a Bruker Invenio spectrometer, operating in the 4000–400 cm^{-1} spectral range. For each measurement, 32 scans were accumulated. The extent of conversion (C%) was calculated by tracking the depletion of the absorption band at 810 cm^{-1}, corresponding to the vinyl C=C twisting vibration, normalized against the invariant internal reference peak at 830 cm^{-1}, assigned to the aromatic C–H vibration, according to equation (1).[21,24]

$$C\% = \left[1 - \frac{\frac{A^{\text{film}}_{810\text{cm}^{-1}}}{A^{\text{film}}_{1930\text{cm}^{-1}}}}{\frac{A^{\text{resin}}_{810\text{cm}^{-1}}}{A^{\text{resin}}_{1930\text{cm}^{-1}}}}\right] \quad (1)$$

^{1}H NMR spectra of TA, GMA and TA-GMx additives were recorded on a Bruker 500-MHz spectrometer in DMSO solvent.

Dynamic-mechanical thermal analysis (DMTA) was performed using an Anton Paar DMA (MCR 702e MultiDrive SN83496752) in rectangular/compression geometry.

Free-standing films for DMTA analysis were obtained by peeling off the cured coating from the ECCS substrate, as described previously. Samples

Table 1: Synthetic conditions of TA-GMx with different TA/GMA molar ratios

Sample	TA:GMx	TA (mmol)	GMA (mmol)	TEA (mmol)	Inhibitor (mmol)	Functionalization degree
TA-GM5	1:5	6.00	30.0	3.40	0.104	4.80
TA-GM15	1:15	6.00	90.0	3.40	0.104	14.9
TA-GM20	1:20	6.00	120.0	3.40	0.104	19.9

Table 2: Composition of the EB-curable formulations

Raw material	Reference formulation (wt%)	Modified formulations (wt%)
Monomer (IBOA)	35	22–20
Co-monomer (CTFA/THFA)	–	12
Tetrafunctional polyester acrylate (resin)	18	18
Bifunctional urethane acrylate (resin)	25	25
Polyester urethane acrylate (resin)	21	21
Acrylated TA additive	–	1–3
Wetting agents	1	1
Average functionality	2.0	2.1–2.4[a]

The calculation of the average functionality was performed using the functionality of TA-GM15 additives

measuring 20 mm × 10 mm were cut from the films. The analysis was carried out from − 50°C to 150°C at a frequency of 1 Hz and a ramp rate of 3°C/min. The storage modulus (E') and the loss factor (tanδ) were recorded as a function of temperature. Glass transition temperature (Tg) was detected as a maximum of the tanδ curve. The ratio between the dissipative modulus (E'') and the storage modulus (E') corresponds to the tanδ, and the maximum of the tanδ can be attributed to Tg. The crosslink density (v_c) was estimated using an equation derived from the statistical theory of rubber elasticity (equation (2)). As this equation approximates the system, it was used only to qualitatively compare the level of crosslinking among the obtained networks.

$$v_c = \frac{E\prime_R}{3RT} \tag{2}$$

where vc is the number of moles of network chains per unit volume of the crosslinked network, E'_R is the storage modulus values in the rubbery plateau region extracted from the graph at 50°C above Tg, R is the gas constant and T is the absolute temperature (i.e., at Tg + 50°C).[26] The test was repeated three times for each formulation.

The adhesion strength between the coatings and the steel substrates was evaluated by cross-hatch adhesion test following the guidelines outlined in ASTM D3359 method B. A cross-cut lattice pattern, comprising six cuts in each direction, was created on the samples using an Elcometer 107 cutter (insert no. 3). The incisions were then covered with a pressure-sensitive tape, which was subsequently rapidly removed from the surface. The substrate's surface was meticulously examined through a magnifying lens to determine the extent of coating removal. The results were classified according to the criteria outlined in Fig. 1, with the use of reference images to facilitate comparison.

The flexibility and adhesion of the coatings under mechanical deformation were evaluated using a wedge bend test in accordance with EN 13523-7. The coated samples were bent over a conical mandrel to form a wedge shape, thereby generating a gradient of tensile stress along the bend. Subsequent to the deformation process, the samples were immersed in a $CuSO_4$ solution to simulate corrosive conditions and to reveal any cracks or porosity that may have developed during the bending process. The degree of coating integrity was determined by measuring the percentage of the film that remained intact along the bend, as calculated using equation (3).

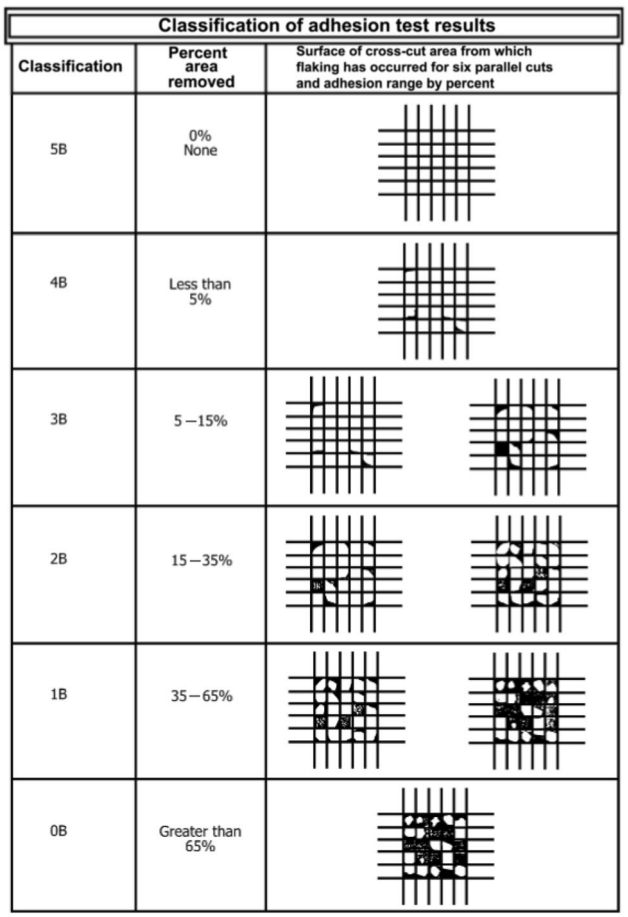

Fig. 1: Classification of adhesion test results in accordance with ASTM D3359-23 standard

$$\%\text{Intact film} = \frac{\text{cracking/porosity}}{\text{total sample length}} * 100 \quad (3)$$

A value above 85% of intact film was considered indicative of satisfactory flexibility and adhesion.

To evaluate the corrosion resistance of the coatings, a cross-cut incision was made on each sample in order to expose the underlying metal substrate. The samples were then immersed in a 0.3 M $CuSO_4$ solution for 4 hours, in order to simulate aggressive environmental conditions exposure. The results of the test were expressed in terms of the extent of the delaminated surface area, representing the portion of the coating that detached or lifted from the substrate after exposure. A smaller delaminated area is indicative of stronger adhesion between the coating and the substrate and, consequently, better overall corrosion protection performance.

Results and discussion

Synthesis and characterization of TA-GMx additives

Three partially acrylated tannic acid derivatives, TA-GMx, with different degrees of acrylation x, were synthesized by reacting TA with GMA (Fig. 2). A mixture of methanol and water was used as the solvent, while triethylamine was employed as the catalyst. BHT was also added to the mixture to inhibit thermal polymerization. The reaction was conducted at 80°C for 24 hours, after which the product was recovered by solvent evaporation and characterized by ^{1}H NMR and FTIR spectroscopy. The products obtained were named TA-GM5, TA-GM15 and TA-GM20, corresponding to molar ratios of TA to GMA of 1:5, 1:15 and 1:20, respectively.

Figure 3a displays the ^{1}H NMR spectra of pristine TA (black), GMA (blue), and the TA–GM15 derivative (red). The TA spectrum exhibits characteristic resonances corresponding to aromatic protons in the region δ = 6.8–7.2 ppm. In the GMA spectrum, distinct signals are observed for the vinyl protons at δ = 5.7–6.1 ppm (*f*), the methylene protons adjacent to the epoxy ring at δ = 3.7–4.5 ppm, the epoxy ring protons themselves at δ = 2.5–3.4 ppm, and the methyl group of the methacrylate moiety at δ = 1.9 ppm. In the spectrum of the TA–GM15 derivative, signals pertaining to the aromatic rings derived from TA are discernible at δ = 6.9–7.1 ppm (a), alongside the characteristic methacrylate peaks: vinyl protons (δ = 5.7–6.1 ppm) (f) and methyl groups (δ = 1.8 ppm). The successful functionalization is further corroborated by the complete disappearance of the epoxide ring signals and the simultaneous emergence of a new peak at δ = 3.7 ppm (h), assigned to the methine proton formed upon ring opening.[21–24]

The ^{1}H NMR spectra of the TA–GMx derivatives, shown in Fig. 3b, confirm the successful synthesis of derivatives with different functionalization degrees. The extent of functionalization was determined by the ratio between integral values of signals derived from the vinyl protons (originating from GMA) and the aromatic protons (originating from TA). Results are summarized in Table 1. These findings suggest that the extent of functionalization of TA-GMx derivatives can be readily modulated by adjusting the TA/GMA feed ratio.

FTIR analysis provided further confirmation of the successful functionalization TA. Figure 4 compares the spectra of pristine TA, GMA and TA–GM15 derivative. The spectrum of unmodified TA displays a broad absorption band between peak 2000 and 3600 cm^{-1}, assigned to hydroxyl groups, along with characteristic signals at 1700 cm^{-1}, corresponding to carbonyl groups, and 1600 cm^{-1}, related to the aromatic ring.

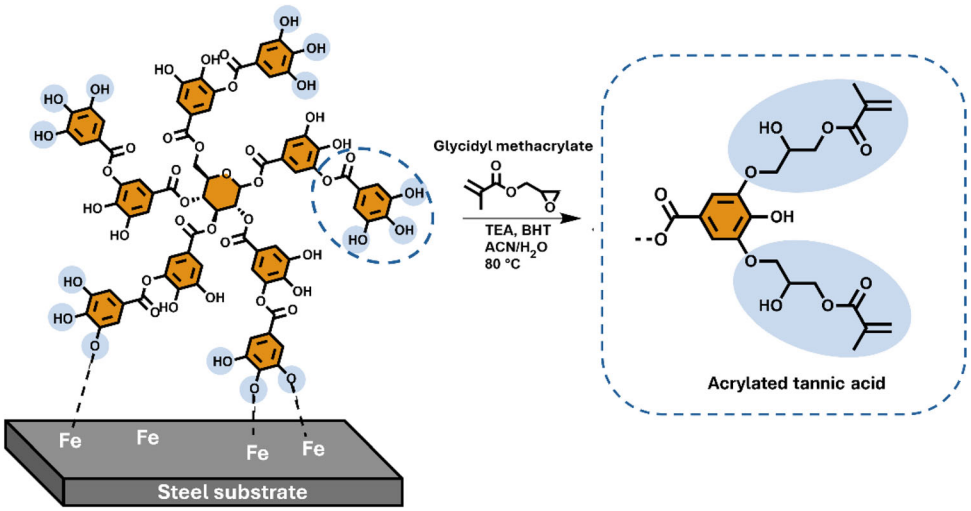

Fig. 2: Schematic of the acrylation process of tannic acid with glycidyl methacrylate

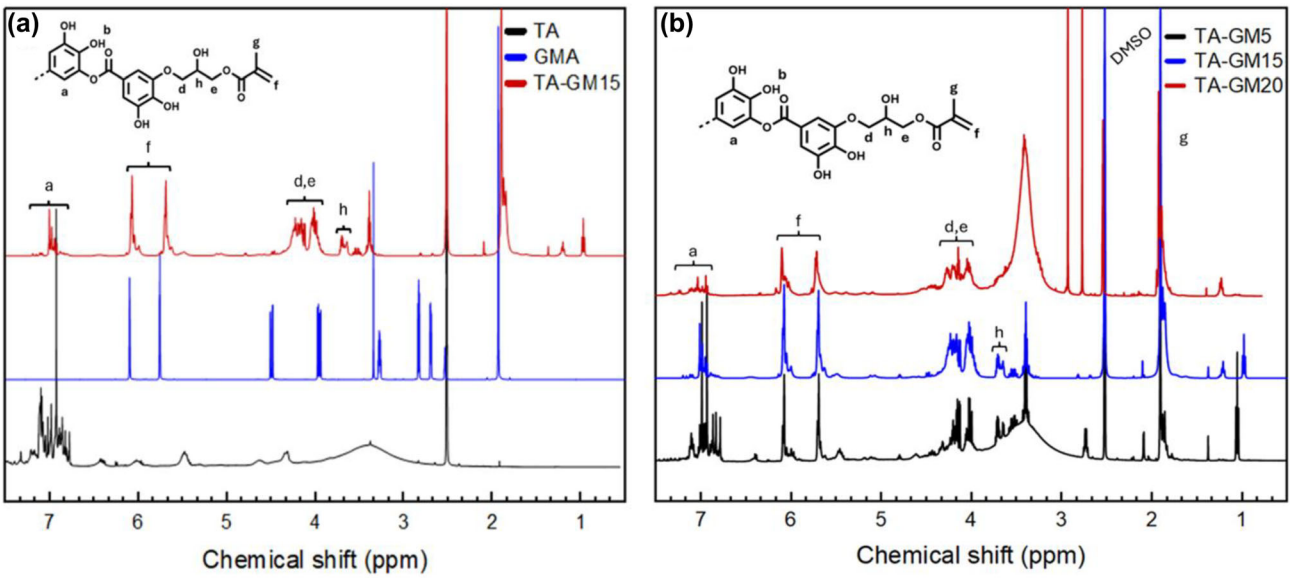

Fig. 3: (a) ^{1}H NMR spectra of TA, GMA and TA-GM15 derivative; (b) ^{1}H NMR spectra of the TA-GM5, TA-GM15 and TA-GM20 derivatives

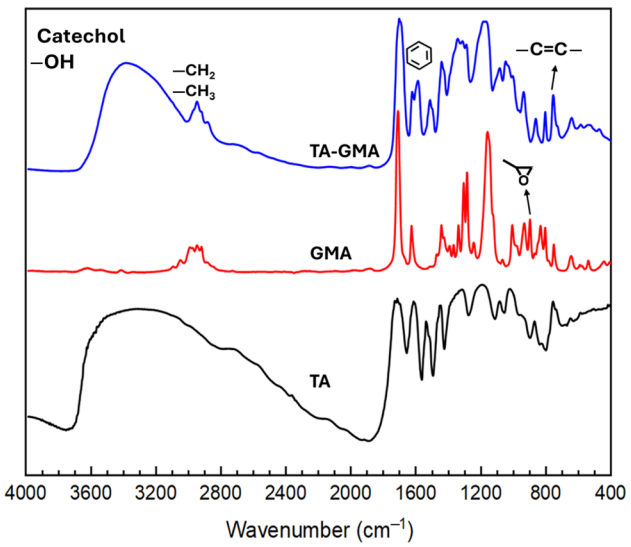

Fig. 4: ATR FTIR spectra of TA, GMA and TA-GM15

In the TA–GM15 spectrum, the hydroxyl band is preserved but noticeably narrows into the 3000 and 3600 cm^{-1} range. This phenomenon is not ascribed to a net loss of hydroxyl functionalities—since the epoxide ring opening reaction generates a new secondary hydroxyl group for every phenolic hydroxyl consumed—but rather to a reduction in intramolecular hydrogen bonding.[24] Furthermore, functionalization is evidenced by the emergence of new absorption bands at 2960 and 2880 cm^{-1}, attributable to the stretching vibrations of the $–CH_3$ and $–CH_2$ groups, and at 1631, 943 and 811 cm^{-1}, attributable to the C=C stretching of the methacrylate moiety.[21]

Compatibility of TA-GMx additives with EB-curable resin

The miscibility of the TA–GMx additives within the EB-curable resin was evaluated to assess their compatibility and the influence of chemical modification on dispersion behavior. The starting point was an EB-curable base formulation provided by the industrial partner, comprising a blend of three different resins and isobornyl acrylate (IBOA) as a reactive diluent (see composition in Table 2). This particular formulation was selected due to its inherently low adhesion to the target metal substrates. Consequently, it serves as an ideal model system to rigorously quantify the adhesion enhancements conferred by the synthesized bio-based additives.

Initial attempts to incorporate TA–GMx additives into the reference formulation at 1 and 3 wt% loadings revealed limited miscibility, particularly for derivatives with lower degrees of acrylation. Despite prolonged mixing (12 h) at 50°C, the mixtures remained turbid and underwent rapid phase separation upon resting, as illustrated in Fig. 5. This instability stems from the marked polarity mismatch between the hydrophilic TA-GMx derivatives and the predominantly apolar components of the resin matrix.

To overcome these solubility constraints, the formulation was modified by introducing polar comonomers (CTFA or THFA) to bridge the compatibility gap. Both comonomers effectively solubilized the TA–GMx additives up to a concentration of 20 wt% (Fig. 6), yielding clear and stable solutions. Consequently, these comonomers were incorporated at a 12 wt% loading, partially replacing IBOA to maintain a constant average functionality in the base system. The TA–GMx additives were then successfully intro-

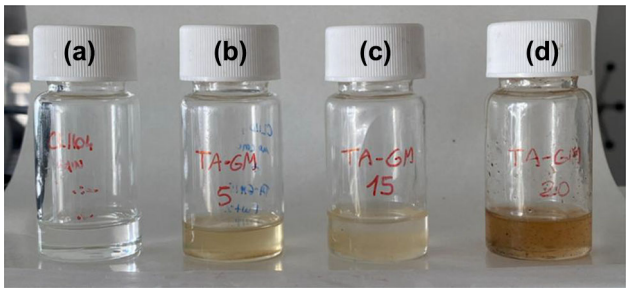

Fig. 5: Digital photographs of the EB-curable formulations: reference formulation without additives (a), modified formulations with TA-GM5 (b), TA-GM15 (c) and TA-GM20 (d)

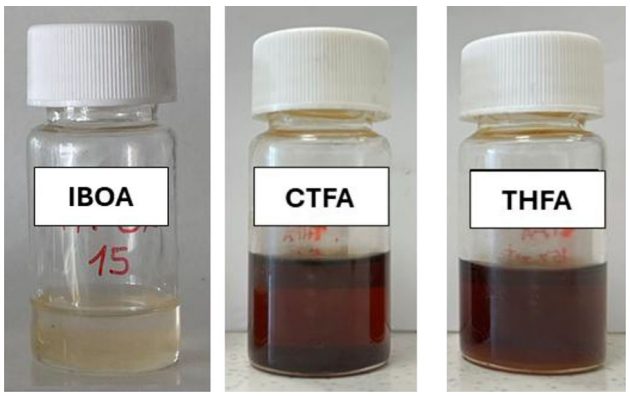

Fig. 6: Solubility tests of TA-GM15 additive in IBOA, CTFA and THFA monomers

duced into this modified formulation at 1 and 3 wt% loading, resulting in calculated average functionalities of 2.1 and 2.4, respectively (based on TA–GM15, as detailed in Table 2).

DMTA analysis of EB-cured films

Figure 7 displays the DMTA analysis for the reference system and the films containing TA–GMx additives. Examination of the rubbery plateau region (Fig. 7a) allows for the calculation of the crosslink density (XLD) of the cured networks. The neat base formulation exhibited an XLD value of 683 mol/m^3. The introduction of TA–GM5 and TA–GM15 at 1 wt% did not significantly alter this parameter, resulting in values of 655 and 675 mol/m^3, respectively.

In contrast, the film containing 1 wt% of TA–GM20 reached the highest XLD of 824 mol/m^3, indicating the formation of a tighter network structure. This enhancement correlates with the higher degree of acrylation in the TA–GM20 derivative, which provides a greater density of reactive methacrylate groups for EB-induced polymerization.[26] The progressive increase in XLD observed from TA–GM5 to TA–GM20 at 1 wt% loading confirms that the substitution of phenolic -OH groups with methacrylate moieties simultaneously increases the number of polymerizable sites and reduces the potential for radical inhibition.[27,28]

However, a comparison between TA–GM15 at 1 wt% and 3 wt% reveals an inverse trend. Despite having the same degree of acrylation, increasing the loading to 3 wt% led to a significant drop in crosslink density (444 mol/m^3). This counterintuitive decrease is attributed to the radical scavenging activity of the residual phenolic groups; at higher concentrations, the inhibitory effect of these moieties becomes predominant, hindering double-bond conversion during the rapid EB curing process.[18]

The tan δ curves (Fig. 7b) further support these observations. The incorporation of TA–GMx additives generally shifts the glass transition temperature (Tg) to slightly higher values compared to the reference formulation (Tg = 71°C), reflecting the increased crosslink density. However, this effect is not particularly pronounced, suggesting that the crosslinked structure is not significantly altered by the addition of TA–GMx additives.

Moreover, TA–GM15 (3 wt%) displays a lower Tg (73°C) than its 1 wt% counterpart, consistent with its lower XLD.

Overall, these results suggest that the modification of the EB-curable network by the TA-GMx additives is governed by a trade-off between two opposing factors: (i) the introduction of additional crosslinking sites, which enhances network density at low loadings, and (ii) the radical scavenging effect of residual phenolic moieties, which becomes predominant at higher loadings, thereby compromising curing efficiency and network homogeneity.

Adhesion performance

The adhesion of the coatings to various metallic substrates was evaluated using the cross-hatch test in accordance with ASTM D3359-23. For this test, we focused exclusively on the TA–GM15 additive, selected for its superior performance in preliminary characterizations.

Results are collected in Table 3, reported on a scale of 0–5 (where 5 indicates excellent adhesion with no detachment and 0 indicates complete coating removal).

The neat reference formulation exhibited negligible adhesion (0–0.5) across all substrates tested, while the incorporation of TA–GM15 additive yielded significant improvements, particularly in formulations containing CTFA as comonomer. Optimal performance was achieved at 1 wt% loading, where excellent adhesion was observed on ETP ox, CFPA, and LTS. This enhancement, reflecting a stronger interaction between the coating and metal surface, can be attributed to the formation of coordination or hydrogen bonds between the additive's catechol/hydroxyl groups and the metal oxide layer.[18]

However, increasing the loading to 3 wt% resulted in a slight performance decline (e.g., to 4–4.5 on ETP

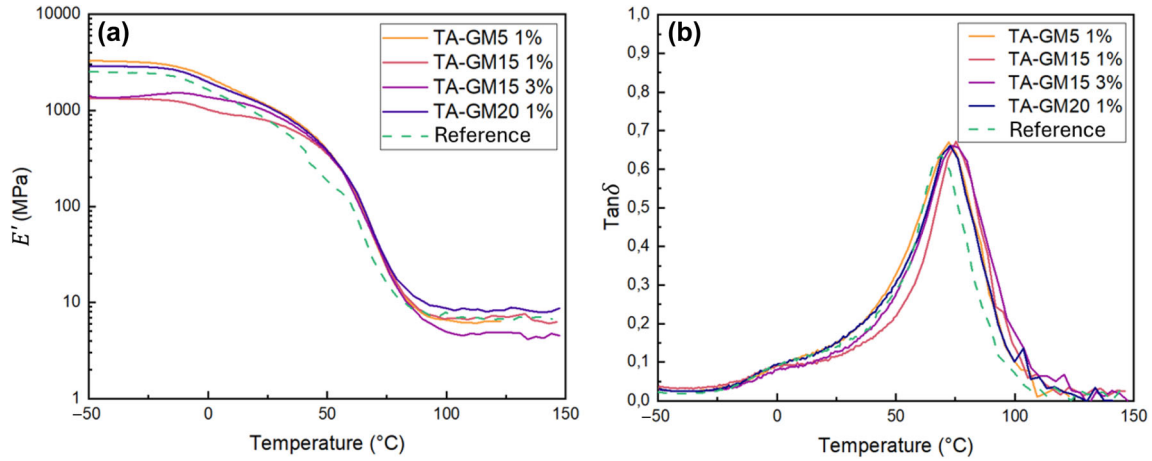

Fig. 7: Storage modulus (E') curves (a) and tanδ (b) curves of EB-cured film obtained from the modified formulations containing TA-GMx additives and the reference formulation without additives

Table 3: Cross-hatch results of the EB-cured coatings with different blends of TA-GM15 on different substrates

	Reference formulation	Blend IBOA/CTFA		Blend IBOA/THFA	
Substrate	No additive	1 wt% additive	3 wt% additive	1 wt% additive	3 wt% additive
ETP	0	3.5	2.5	2	1.5
ETP ox	0.5	5	4.5	4.5	4
CFPA	0	5-	4.5	5	4
LTS	0	5-	4	2.5	2.5

ox and CFPA). This suggests that excessive additive levels may induce micro-phase separation or interfacial stress accumulation, thereby disrupting the delicate balance between cohesion and adhesion.

Comparing the comonomer blends, IBOA/CTFA consistently outperformed IBOA/THFA, with the latter reaching a maximum score of 5 only on CFPA (1 wt%). The inferior performance of THFA is likely due to its higher polarity and lower flexibility, which hinder substrate wetting and interfacial interpenetration, limiting mechanical interlocking and adhesion strength.

Flexibility and adhesion under mechanical deformation were assessed via the wedge bend test (EN 13523-7). The percentage of intact film was calculated as described in the experimental session, with values above 85% indicating satisfactory coating integrity.

As detailed in Table 4, the addition of TA–GM15 additive significantly enhanced coating integrity, raising the percentage of intact film from 75 to 80% (reference formulation) to 86–92.5% (IBOA/CTFA, 1 wt%), surpassing the satisfactory threshold of 85% across all substrates tested. This demonstrates the additive's ability to improve cohesive deformation and inhibit crack initiation during bending.

Consistent with static adhesion results, the 1 wt% formulations outperformed the 3 wt% samples. For instance, on ETP ox, integrity dropped from 92.5% (1 wt%) to 90% (3 wt%). This trend aligns with the reduced crosslinking efficiency observed in DMTA analysis, suggesting that excessive loading disrupts the optimal network architecture. Furthermore, the IBOA/CTFA blend proved superior, achieving up to 92.5% integrity compared to the 91% (CFPA) and 84% (ETP ox) obtained with the THFA-based system.

Overall, 1 wt% TA–GM15 in the IBOA/CTFA blend represents the optimal formulation, striking the best balance between crosslink density, flexibility, and strong interfacial bonding.

Corrosion test

Robust interfacial adhesion is widely recognized as a critical factor governing the corrosion resistance of protective coatings. To evaluate the effectiveness of the TA–GM15 additive in corrosion protection, accelerated corrosion tests were performed on CPFA substrates. The reference formulation was systematically compared with modified formulations incorporating either THFA or CTFA as comonomers, in order to assess their relative performance. For each formulation, TA–GM15 was introduced at two different loadings (1 and 3 wt%), allowing the influence of

Table 4: Wedge bend results of the EB-cured coatings with different blends of TA-GMx additives on different substrates

	Reference formulation	Blend IBOA/CTFA		Blend IBOA/THFA	
Substrate	No additive	1 wt% additive	3 wt% additive	1 wt% additive	3 wt% additive
ETP	75	86	85	79	80
ETP ox	79	92.5	90	84	82
CFPA	80	90	90	91	88
LTS	78	89	86	80	81

additive concentration to be evaluated. Coated samples were cross-cut and immersed in a $CuSO_4$ solution for four hours to simulate aggressive conditions, allowing for the evaluation of coating integrity and resistance to delamination and electrolyte undercutting. Performance was rated on a scale of 0–5 (where 5 denotes no defects and 0 indicates complete failure), using a standard commercial solvent-based coating as a benchmark.

As illustrated in Fig. 8 and Table 5, the incorporation of TA–GM15 substantially enhanced corrosion resistance across all systems compared to the additive-free reference formulation.

The IBOA/CTFA system exhibited superior performance, achieving a rating of 4.5 at 1 wt% loading, compared to 3.75 for the neat blend. Conversely, the IBOA/THFA blend showed a modest yet significant improvement (from 2.0 to 3.5 at 1 wt%). Its inferior performance relative to IBOA/CTFA suggests that THFA's higher polarity may hinder substrate wetting, thereby creating interfacial defects that compromise protection. Consistent with previous results, increasing the additive concentration to 3 wt% led to a slight decline in performance in both systems.

Notably, the optimal EB-cured formulation (IBOA/CTFA, 1 wt%) demonstrated corrosion resistance comparable to the solvent-based benchmark (rating 4.5 vs 4.75). In stark contrast, the unmodified reference formulation yielded the poorest results (rating 2.0), underscoring the pivotal role of TA–GM15 additive in developing sustainable, high-performance metal packaging coatings.

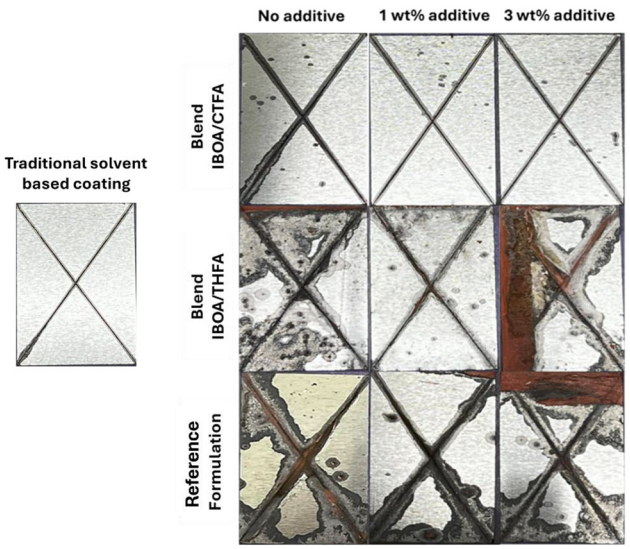

Fig. 8: Digital photos of Cr-free tin plate coated with reference and modified formulations after 4 h in a copper sulfate solution

Conclusions

This study successfully validates the potential of partially acrylated tannic acid derivatives (TA–GMx) as bio-based adhesion promoters for high-performance EB-curable coatings in metal packaging applications. Through the reaction with glycidyl methacrylate, tannic acid was effectively functionalized with precise control over the obtained functionality. The integration of these derivatives into an industrial formulation required the use of specific polar comonomers (CTFA or THFA), which proved essential for ensuring adequate miscibility and preventing phase separation. The incorporation of TA–GMx additives yielded substantial improvements in coating performance across all investigated metallic substrates, particularly regarding adhesion, post-deformation flexibility, and corrosion resistance. Optimal performance was identified at low loadings (1 wt%), where a critical balance was struck between enhancing interfacial interactions and maintaining efficient network formation. At this concentration, a synergistic mechanism was observed: the catechol-rich core of the additive provided strong anchoring to the metal surface via coordination bonding, while the introduced acrylate groups ensured covalent integration into the polymer network during EB curing.

Most notably, the optimized EB-cured system (IBOA/CTFA with 1 wt% TA–GMx) demonstrated performance levels comparable to a conventional solvent-based, thermally cured benchmark. This finding is of significant industrial relevance, as it highlights the feasibility of replacing energy-intensive thermal processes with sustainable, solvent-free EB technology

Table 5: Corrosion results of the EB-cured coatings with different blends of TA-GMx additives on Cr-free substrates

Cr-free substrate

Formulation	No additive	1 wt% additive	3 wt% additive
Commercial solvent-based	4.75	–	–
Blend IBOA/CTFA	3.75	4.5	4
Blend IBOA/THFA	2	3.5	3
Reference formulation	2	–	–

without sacrificing functional quality. Consequently, the combination of EB curing and bio-based adhesion promoters emerges as a viable, eco-efficient strategy for the next generation of food metal packaging coatings.

Funding Open access funding provided by Università degli Studi del Piemonte Orientale Amedeo Avogrado within the CRUI-CARE Agreement. MUR is acknowledged for funding F. Bisio's Ph.D. fellowship (MUR D.M.118/2023—Borse dottorati generici ricerca PNRR). METLAC S.p.A. is acknowledged for the collaboration and funding.

Data availability The data that support the findings of this study are available from the corresponding author upon reasonable request.

Conflict of interest The authors declare that they have no conflict of interest.

References

1. Datta, SK, Chaki, TK, Bhowmick, AK, "Electron Beam Processing of Polymers." In: *Advanced Polymer Processing Operations*, pp 157–186. Elsevier (1998)
2. Crivello, JV, "Advanced Curing Technologies Using Photo- and Electron Beam Induced Cationic Polymerization." *Radiat. Phys. Chem.*, **63** 21–27. https://doi.org/10.1016/S0969-806X(01)00476-5 (2002)
3. Saunders, C, Lopata, V, Barnard, J, Stepanik, T, "Electron Beam Curing Taking Good Ideas to the Manufacturing Floor." *Radiat. Phys. Chem.*, **57** 441–445. https://doi.org/10.1016/S0969-806X(99)00411-9 (2000)
4. Sheel Wali, A, Kumar, S, Khan, D, "A Review on Recent Development and Application of Radiation Curing." *Mater. Today. Proc.*, **82** 68–74. https://doi.org/10.1016/j.matpr.2022.11.342 (2023)
5. Aparicio, JL, Elizalde, M, "Migration of Photoinitiators in Food Packaging: A Review." *Packag. Technol. Sci.*, **28** 181–203. https://doi.org/10.1002/pts.2099 (2015)
6. Wei, Z, Wang, L, Liu, R, Luo, J, "Irradiation-cured Graphene Composite Films: A Comparison Between UV and EB Curing." *J. Coat Technol. Res.*, **20** 1713–1726. https://doi.org/10.1007/s11998-023-00776-5 (2023)
7. Manfredi, LB, Ginés, MJL, Benítez, GJ, et al. "Use of Epoxy–Phenolic Lacquers in Food can Coatings: Characterization of Lacquers and Cured Films." *J. Appl. Polym. Sci.*, **95** 1448–1458. https://doi.org/10.1002/app.21389 (2005)
8. Aydemir, C, Özsoy, SA, "Environmental Impact of Printing Inks and Printing Process." *J. Graph. Eng. Des.*, **11** 11–17 (2020). https://doi.org/10.24867/JGED-2020-2-011
9. Schissel, SM, Jessop, JLP, "Quantitative Comparison of Photo- and Electron-beam Polymerizations Based on Equivalent Initiation Energy." *Radiat. Phys. Chem.*, **157** 72–83. https://doi.org/10.1016/j.radphyschem.2018.12.023 (2019)
10. Lestido-Cardama, A, Sendón, R, Bustos, J, et al. "Food and Beverage can Coatings: A Review on Chemical Analysis, Migration, and Risk Assessment." *Compr. Rev. Food Sci. Food Saf.*, **21** 3558–3611. https://doi.org/10.1111/1541-4337.12976 (2022)
11. Sathyanarayana, MN, Yaseen, M, "Role of Promoters in Improving Adhesions of Organic Coatings to a Substrate." *Prog. Org. Coat.*, **26** (2–4) 275–313 (1995)
12. Walker, P, "Organosilanes as Adhesion Promoters." *J. Adhes. Sci. Technol.*, **5** 279–305. https://doi.org/10.1163/156856191X00369 (1991)
13. Mikić, D, Radovanović-Perić, F, Otmačić Ćurković, H, "Phosphonic Acids as Corrosion Inhibitors and Adhesion Promoters for Organic Coatings and Bronze." *Materials*, **17** 3710. https://doi.org/10.3390/ma17153710 (2024)
14. Wang, X, Zhang, J, Liu, J, Luo, J, "Phytic Acid-based Adhesion Promoter for UV-curable Coating: High Perfor-

mance, Low Cost, and Eco-friendliness.'' *Prog. Org. Coat.*, **167** 106834. https://doi.org/10.1016/j.porgcoat.2022.106834 (2022)
15. Lee, H, Lee, BP, Messersmith, PB, ''A Reversible Wet/Dry Adhesive Inspired by Mussels and Geckos.'' *Nature*, **448** 338–341. https://doi.org/10.1038/nature05968 (2007)
16. Manolakis, I, Azhar, U, ''Recent Advances in Mussel-Inspired Synthetic Polymers as Marine Antifouling Coatings.'' *Coatings*, **10** 653. https://doi.org/10.3390/coatings10070653 (2020)
17. Guo, Q, Chen, J, Wang, J, et al. ''Recent Progress in Synthesis and Application of Mussel-inspired Adhesives.'' *Nanoscale*, **12** 1307–1324. https://doi.org/10.1039/C9NR09780E (2020)
18. Hosseini, M, Moghaddam, L, Barner, L, et al. ''The Multifaceted Role of Tannic Acid: From Its Extraction and Structure to Antibacterial Properties and Applications.'' *Prog. Polym. Sci.*, **160** 101908. https://doi.org/10.1016/j.progpolymsci.2024.101908 (2025)
19. Xu, Z, ''Mechanics of Metal-Catecholate Complexes: The Roles of Coordination State and Metal Types.'' *Sci. Rep.*, **3** 2914. https://doi.org/10.1038/srep02914 (2013)
20. Yan, G, Chen, G, Peng, Z, et al. ''The Cross-Linking Mechanism and Applications of Catechol-Metal Polymer Materials.'' *Adv. Mater. Interfaces*, **8** 2100239. https://doi.org/10.1002/admi.202100239 (2021)
21. Sesia, R, Cardone, AG, Ferraris, S, et al. ''Exploitation of Tannic acid as Additive for the Adhesion Enhancement of UV-curable Bio-based Coating.'' *Prog. Org. Coat*, **189** 108311. https://doi.org/10.1016/j.porgcoat.2024.108311 (2024)
22. Liu, R, Zheng, J, Guo, R, et al. ''Synthesis of New Biobased Antibacterial Methacrylates Derived from Tannic Acid and Their Application in UV-Cured Coatings.'' *Ind. Eng. Chem. Res.*, **53** 10835–10840. https://doi.org/10.1021/ie501804p (2014)
23. Liu, R, Zhu, J, Luo, J, Liu, X, ''Synthesis and Application of Novel UV-Curable Hyperbranched Methacrylates from Renewable Natural Tannic Acid.'' *Prog. Org. Coat*, **77** 30–37. https://doi.org/10.1016/j.porgcoat.2013.07.015 (2014)
24. Wang, X, Zhang, J, Liu, J, et al. ''Synthesis of Acrylated Tannic Acid as Bio-based Adhesion Promoter in UV-curable Coating with Improved Corrosion Resistance.'' *Coll. Surf. Physicochem. Eng. Asp.*, **644** 128834. https://doi.org/10.1016/j.colsurfa.2022.128834 (2022)
25. Sesia, R, Rodríguez, Pou I, P, Calovi M, et al. ''Microwave-Functionalized Natural Tannic Acid as an Anticorrosive UV-curable Coating.'' *Polymer*, **315** 127824. https://doi.org/10.1016/j.polymer.2024.127824 (2024)
26. Frison, T, Seegers, WJM, Totev, DI, Esteves, ACC, ''Insights on Chemical Reactions and Formation Process of Electron Beam-Cured Acrylic Networks.'' *Macromolecules*, **57** 1291–1301. https://doi.org/10.1021/acs.macromol.3c02085 (2024)
27. Lopes, GKB, Schulman, HM, Hermes-Lima, M, ''Polyphenol Tannic Acid Inhibits Hydroxyl Radical Formation from Fenton Reaction by Complexing Ferrous Ions.'' *Biochim. Biophys. Acta. BBA – Gen. Subj.*, **1472** 142–152. https://doi.org/10.1016/S0304-4165(99)00117-8 (1999)
28. He, Y, Li, N, Xiang, Z, et al. ''Natural Polyphenol as Radical Inhibitors Used for DLP-based 3D Printing of Photosensitive Gels.'' *Mater. Today Commun.*, **33** 104698. https://doi.org/10.1016/j.mtcomm.2022.104698 (2022)